Neuron, Vol. 18, 599–612, April, 1997, Copyright ©1997 by Cell Press

Heterogeneous Release Properties of Visualized Individual Hippocampal Synapses

Venkatesh N. Murthy*†, Terrence J. Sejnowski,* and Charles F. Stevens†
*Computational Neurobiology Laboratory
†Molecular Neurobiology Laboratory
Howard Hughes Medical Institute
Salk Institute
La Jolla, California 92037

Summary

We have used endocytotic uptake of the styryl dye FM1–43 at synaptic terminals (Betz and Bewick, 1992) to study properties of individual synapses formed by axons of single hippocampal neurons in tissue culture. The distribution of values for probability of evoked transmitter release *p* estimated by dye uptake is continuous, with a preponderance of low *p* synapses and a broad spread of probabilities. We have validated this method by demonstrating that the optically estimated distribution of *p* at autapses in single-neuron microislands predicts, with no free parameters, the rate of blocking of NMDA responses by the noncompetitive antagonist MK–801 at the same synapses. Different synapses made by a single axon exhibited varying amounts of paired-pulse modulation; synapses with low *p* tended to be facilitated more than those with high *p*. The increment in release probability produced by increasing external calcium ion concentration also depended on a synapse's initial *p* value. The size of the recycling pool of vesicles was strongly correlated with *p* as well, suggesting that synapses with higher release probabilities had more vesicles. Finally, *p* values of neighboring synapses were correlated, indicating local interactions in the dendrite or axon, or both.

Introduction

The reliability and effectiveness of communication between neurons is governed by fundamental properties of synapses and, in most cases, these properties are inferred from responses of synapse populations. However, population characteristics can obscure important differences between individual synapses. For instance, release probability *p* (that is, the probability that at least one quantum will be released when a nerve impulse arrives) in some areas of the brain appears to be quite low and variable across synapses (Hessler et al., 1993; Rosenmund et al., 1993; Allen and Stevens, 1994; Stevens and Wang, 1994), although this dominant feature of synaptic transmission is not apparent in currents generated by a population of synapses. The study of individual synapses is important, then, but only a few techniques are available for investigating single synapse properties.

The methods of minimal stimulation and cell pair stimulation–recording have been used to isolate putative single synapses and investigate their properties in a few instances (Raastad et al., 1992; Stevens and Wang, 1994, 1995; Bolshakov and Siegelbaum, 1995). These methods, however, require multiple criteria to be satisfied to increase the likelihood that a single synapse is being activated, are prone to misinterpretation, and yield data reluctantly. In addition, the minimal stimulation or cell pair techniques necessitate pooling data from multiple slices and animals in order to compare the properties of one synapse with another. Even the apparently most direct method of studying individual synapse properties with paired recordings from connected cells does not guarantee that single synapses are being investigated—multiple contacts reportedly occur almost always between cortical neuron pairs (Thomson et al., 1993).

We have used the method pioneered by Betz and collaborators (Betz and Bewick, 1992; Betz et al., 1992), and recently extended to central synapses in culture (Ryan et al., 1993, 1996a; Ryan and Smith, 1995), to investigate various characteristics of the individual synapses made by a single neuron. When synaptic boutons are stimulated in the presence of the styryl dye FM1–43, exocytosed synaptic vesicles take up the dye during recovery of the vesicular membrane. After washing with dye-free medium, fluorescence is observed in puncta corresponding to synaptic terminals that were active when the dye was present (Ryan et al., 1993; Ryan and Smith, 1995; Henkel et al., 1996). Synaptic properties can then be determined by measuring the fluorescence intensity and its changes with synaptic use and other variables.

In the present study, individual synapses were identified by their location, and the uptake and release of the fluorescent dye permitted us to estimate the release probability, paired-pulse facilitation and depression, synaptic strength as a function of extracellular calcium concentration, and the size of the recycling vesicular pool for specific members of a relatively large population of synapses made by single hippocampal neurons in culture. We find that these properties are heterogeneous across the population but that they are highly correlated at individual synapses. Most synapses have a release probability of <0.3 that is stable over time, but specific synapses can exhibit probabilities that range from <0.05–0.9 or more. Neighboring synapses on the same dendrite tend to have similar release probabilities. Paired-pulse facilitation is extremely variable from synapse to synapse but is highly correlated with release probability, with the less reliable synapses showing the largest facilitation, and synapses with a release probability $>\sim 0.5$ exhibiting little or no facilitation. Increasing extracellular calcium concentration causes an increment in release probability as expected, but again, the largest effect is on the lower probability synapses. The size of the total vesicular pool also varies from synapse to synapse but is highly correlated with release probability, as if the larger synapses are the most reliable.

Results

Theory for FM1–43 Labeling and Destaining

We have used a simple theory to estimate release probabilities *p* (see Appendix): release probability is taken to

be the fraction of the stimuli that result in an endocytotic event. This works because exocytosis and endocytosis are closely matched (Heuser and Reese, 1973; Von Gersdorff and Matthews, 1994; Smith and Betz, 1996) and because hippocampal synapses generally release at most one vesicle per nerve impulse (Stevens and Wang, 1994, 1995). If synapses are labeled by evoking *i* presynaptic action potentials in the presence of FM1–43, then for each bouton, the release probability *p* is given by

$$p = \frac{F_i}{ci} \tag{1}$$

where F_i is the fluorescence intensity of the bouton after *i* stimuli, and *c* is a factor that corresponds to the average fluorescence intensity of a single vesicle; thus, F_i/c is the number of endocytosed vesicles, and *p* is the ratio of this number to the total number of stimuli.

After labeling, the fluorescent puncta are subsequently destained by a long train of action potentials. If $\hat{F}_0$ represents the initial fluorescence after loading (before the onset of the destaining stimulus), and $\hat{F}_k$ is the fluorescence after *k* destaining action potentials, we can derive the following relation (see Appendix)

$$\frac{p}{N} = \frac{1}{k}\left(1 - \frac{\hat{F}_k}{\hat{F}_0}\right), \tag{2}$$

where *N* is the average number of vesicles available for release at a given synapse. *N* includes the immediately releasable vesicles and the reserve pool (Rosenmund and Stevens, 1996). For the purpose of our analysis, *N* is the size of the vesicle pool into which newly endocytosed vesicles mix. By taking the ratio of the right-hand sides of equations (1) and (2), we obtain an estimate for *N*:

$$N = \frac{F_i k}{ci\left(1 - \frac{\hat{F}_k}{\hat{F}_0}\right)} \tag{3}$$

Release Probabilities Estimated from Fluorescence Intensities

Distribution of Fluorescence Intensities for Puncta

The goal of the first experiments described here is to determine the distribution of release probabilities for a single neuron's synapses. We use equation (1) (see Appendix) and estimate release probabilities from vesicle staining with stimulus trains.

Figure 1A illustrates a typical image obtained after evoking 20 action potentials (the loading stimulus train) in a neuron at a rate of 0.5 Hz in the presence of 10 μM FM1–43. The preparation remained in the dye for 30 s after the end of the loading stimulus train to provide time for completion of endocytosis (see Experimental Procedures) and was then washed for 6 min with dye-free solution. Numerous localized bright spots of varying intensities are seen. Ryan et al. (1993) have previously shown that these bright spots coincide with presynaptic boutons as determined immunocytochemically, and Henkel et al. (1996) have demonstrated that the dye is localized in vesicles. All analysis presented here includes only isolated spots and not extended bright regions (which are rare). Since only the cell attached to the patch pipette was stimulated during loading of dye, and synaptic blockers were routinely included to prevent recurrent excitation, only the presynaptic release sites of the recorded neuron should be stained except for occasional weak staining arising from spontaneous release.

To confirm that the fluorescent spots indeed corresponded to release sites, and to exclude labeling of synapses by spontaneous activity in cells other than the one under study, action potentials were evoked in the soma to cause release of dye-filled vesicles. Figure 1C shows destaining curves for a typical subset of boutons (only a subset is shown for clarity) stained by a train of action potentials evoked in a single neuron. After four images were acquired (one every 15 s) without stimulation, action potentials were evoked using the patch pipette at a rate of 5 Hz. The fluorescence intensity in almost all bright spots declined. After further acquisition of three images, the neuron was stimulated at 5 Hz for 120 s to completely release all stained vesicles from the boutons, and three further images were obtained to get the final levels of fluorescence. The total amount of releasable fluorescence at each bouton was defined as the difference between the initial fluorescence (averaged over the first four images) and the final fluorescence (averaged over the last three images). Any residual fluorescence left after the extended stimulation was assumed to be nonspecific and nonreleasable and was subtracted from the rest of the images. In most experiments, this residual fluorescence was $<$10% of the background fluorescence.

The distribution of fluorescence intensity for all isolated bright spots that subsequently destained during one experiment (the one in Figure 1) is shown in Figure 2A. According to equation (1), this fluorescence is directly proportional to release probability, and the proportionality constant is the number of stimuli used during the loading procedure (*i*) multiplied by the fluorescence of a single stained vesicle (*c*).

Fluorescence Intensity of Single Vesicles

To convert the distribution of fluorescence intensities (Figure 2A) into release probabilities, we must estimate the proportionality constant *c*, the average fluorescence of a single stained vesicle. For the Figure 2 experiment, evenly spaced fluorescence peaks in the intensity histograms could be discerned at low values of fluorescence when the low intensity region of the histogram was recalculated with smaller bin sizes (Figure 2A for loading [top inset]—destaining—reloading [bottom inset]). We interpret these peaks as corresponding to fluorescence from integral numbers of stained vesicles so that *c* is given by the spacing between peaks. Note that the lowest histogram peak corresponds to boutons with two stained vesicles because puncta with fluorescence values below 140 intensity units (see Experimental Procedures for definition of "intensity units") were excluded. We excluded these dimmest puncta because destaining could not be detected unambiguously for most boutons that started out with very low intensities.

This estimate of *c* could involve two sorts of errors: (1) the peaks may be the result of a statistical artifact (Are the peaks reliable?); and (2) the peaks may be real but correspond not to individual vesicles but rather arise

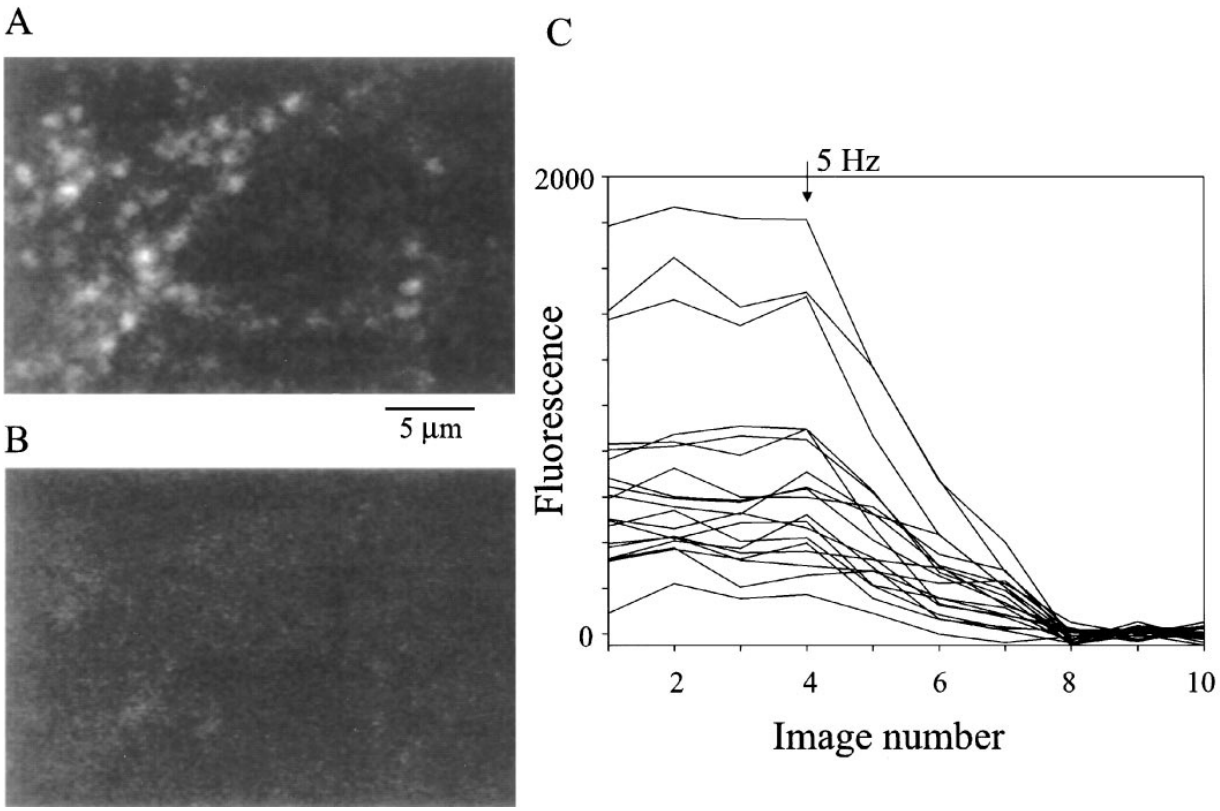

Figure 1. Staining of Synaptic Terminals with FM1–43 and Subsequent Destaining

(A) Fluorescence image of a field of dendritic processes with bright spots corresponding to presynaptic terminals. 20 action potentials were evoked at 0.5 Hz in the presence of 10 μM FM1–43 in the bathing solution. The image was acquired after 6 min of washing in dye-free medium.

(B) Same field after stimulating the neuron in the absence of dye at 5 Hz for >3 min. Practically all the fluorescence is lost.

(C) Fluorescence intensity of 18 representative spots as a function of image number. Images one to four were obtained after labeling the terminals and washing for 6 min. After image four was obtained, the neuron was stimulated at 5 Hz. Note the gradual loss of fluorescence over the next three images. Image acquisition was stopped after image seven, and the cell was continually stimulated for 2 more min to release all labeled vesicles. Images 8–10 were acquired after this prolonged stimulation. The final fluorescence for each spot was subtracted from all other images. Fluorescence units correspond to the integral of the pixel values in the ROI (single pixel intensity varied between 0 and 255).

from some unidentified source of quantization (Is the interpretation of the peaks valid?) We consider these questions in turn.

(1) The number of intensity observations in one of the histograms used to determine c is usually $\sim$30, and each of these observations is a bouton intensity averaged over four frames so a total of $\sim$120 bouton images is used to calculate a histogram. Histograms with such small numbers of entries can display peaks even when the underlying distribution is uniform. Occasionally, the peaks might be as prominent as those in the Figure 2A insets with approximately equal spacing, although Monte Carlo simulations indicate that this would be very rare, particularly for repeated independent determinations as shown in the two Figure 2A insets. To investigate the reliability of the peaks, we determined the peak spacing for eight separate experiments. The average peak separation for these eight experiments is 102 intensity units (SEM = 12; range = 84–117). Thus, the spacing of the peaks appears to be reliable across experiments.

Another check on the reliability of the peaks involves fitting the probability density $p(f)$ (given in the Appendix) to our data. In our experiments, the dominant source of variability that accounts for the spread around the peaks is measurement errors arising from fluctuations in laser power. From a direct determination of this error source, one can predict (see Appendix) that intensities are distributed around each peak according to a Gaussian with a coefficient of variation θ of 0.085. The smooth curves in the Figure 2A insets are the function $p(f)$ with an SD given by the $\theta = 0.085$ determined from the measurement errors. Clearly, the spread of the observations around the peaks is consistent with this prediction.

Data from four experiments were combined to obtain a pooled histogram (the four data sets were chosen based on proximity of experimental dates and the fact that the same batch of experimental solutions were used). A maximum likelihood procedure was used to obtain the parameters (c and w_n) for the function $p(f)$. The variance (σ^2) was determined as described in the Appendix. The best fit of $p(f)$ to the data was compared with two alternatives: (1) a staircase density function (no peaks) and (2) a weighted sum of Gaussian densities with a variance large enough to obscure peaks. The fit

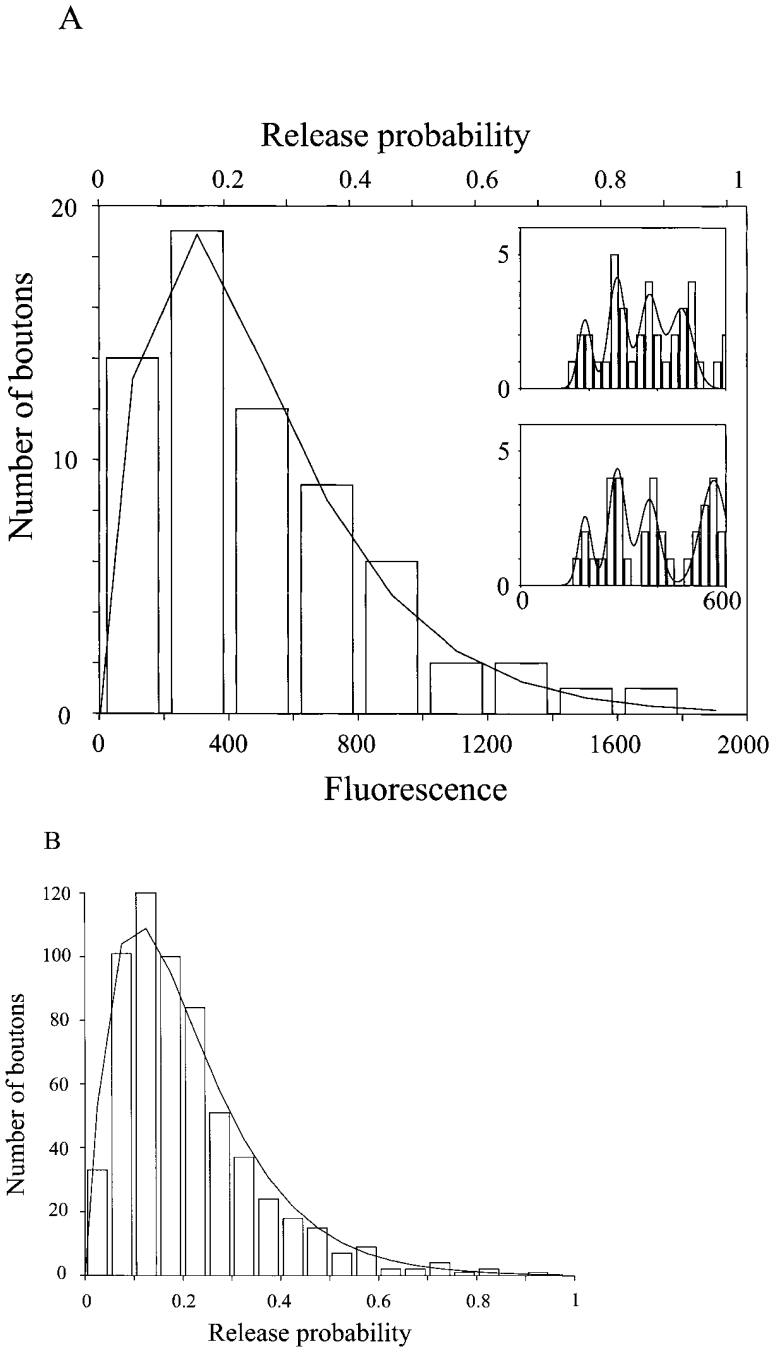

Figure 2. Distribution of Fluorescence Intensities and Release Probabilities at Multiple Boutons of a Single Axon

(A) Histogram of fluorescence intensities for 66 boutons from the cell shown in Figure 1, following stimulation of 20 action potentials. The fluorescence intensity for each bouton was determined by the difference between the average over the first four images and the final three images (see Figure 1C). The histogram is well fitted by Γ (2, λ) with λ = 7.9 (continuous line). To estimate the fluorescence of a single vesicle, the histogram was recalculated with a smaller bin size after the first loading (top inset) and after destaining and reloading (bottom inset). The average distance between the peaks was 94 units and is taken to correspond to the fluorescence of a single vesicle. When fluorescence is scaled using this factor, the values for release probability are obtained and are shown at the top. (B) Histogram of release probabilities for 611 boutons from seven cells grown in vitro for 11–15 days. Raw fluorescence measurements were converted to release probability using the values of *c* estimated as in Figure 2A except for two cells for which *c* was taken to be 102. Solid line is a Γ (n, λ) density function with n = 2, and λ = 11.1.

with the function *p(f)* was >40 times more likely than either of the alternatives.

Taken together, these observations provide strong support for the reliability of the estimates of *c*.

(2) We have evaluated the validity of our interpretation of *c* in three ways. First, we have placed upper and lower limits on the intensity expected for a single vesicle and shown that our estimates fall within this range. Second, we have investigated the intensity expected for staining a structure the size of a synaptic vesicle to show that our estimate is plausible. Third, we have checked the estimates of release probabilities that depend on the value of *c* by an independent method. The first two checks are described here, and the third is considered in the next section.

Limits can be placed on the value of *c* because the dimmest puctum should have at least one stained vesicle, and the brightest punctum should not have more stained vesicles than the number of stimuli used for loading; note that this last statement assumes Katz's N_s = 1 (N_s is the number of Katz release sites/bouton) for all boutons and that few spontaneous releases occurred. The assumption N_s = 1 is based on physiological experiments (Stevens and Wang, 1994, 1995) that found

only single releases or failures at putative single hippocampal synapses and the Schikorski and Stevens (unpublished data) report that the majority of boutons have only a single active zone. If multiple vesicles are released per stimulus, or if significant spontaneous release occurs, the true value of c must be smaller than the estimate of the lower limit given by the brightest puncta.

If the brightest puncta in the Figure 2A experiment correspond to synapses with release probability $p = 1$, so the number of stained vesicles would nearly equal the number of loading stimuli, then $c = max(F_i)/i = 92$, where i is the number of stimuli in the loading train. Alternately, if the dimmest puncta included in our sample contain just one labeled vesicle, then $c = min(F_i) = 145$. Thus $92 < c < 145$; recall for the Figure 2A experiment that $c = 94$.

To check the plausibility of our value for c, we have estimated the fluorescent intensity that might be expected for the stained surface area of membrane provided by a single vesicle. The idea is to stain surface membrane, measure the fluorescence of a known area, and then calculate the fluorescence of a membrane area in a single vesicle. This calculation is quite uncertain because we have no way of estimating the effect of the particular membrane environment provided by a vesicle on the fluorescence of FM1–43, but at least we should be able to decide whether our value for c is of the order of magnitude expected.

We estimated the average fluorescence per unit area of membrane by staining neuronal processes with solution containing a low concentration of FM1–43 (0.5 μM) that was continuously present in the bathing solution. Surface membranes were stained with the dye, and the intensity of the stain, measured in six regions, averaged 696 ($\pm$46) units per μm^2 for 0.5 μM FM1–43; if we suppose dye partitioning is linear between the bath and the membrane, we would expect a fluorescence intensity of $696 \times 20/\mu m^2$ for the 10 μM FM1–43 used for vesicle staining. Assuming an average diameter of 35.2 nm for synaptic vesicles (Schikorski and Stevens, unpublished data), we estimate the fluorescence of a single vesicle would be about 54 intensity units. Although this estimate is likely to be inaccurate, it shows that the value of c obtained above (94) is plausible.

These checks, together with the cross validation of our procedure with the MK–801 method (described later), provide strong support for the validity of our interpretation of c as the average fluorescence of a single stained vesicle.

Distribution of Release Probabilities for a Single Neuron

We chose to use the spacing between peaks (Figure 2A insets) as the scaling factor for the cell in Figure 2A since these peaks appeared at the same positions upon restaining the same set of boutons. When the distribution of F_i is scaled using this factor (c= 94 intensity units), we get the histogram of release probabilities p (top axis of Figure 2A).

Several key features of the distribution should be noticed. First, the distribution is broad, with a coefficient of variation >50%. Second, the distribution appears to be continuous rather than, say, bimodal with two populations of synapses, one with high p and one with low p. Third, the distribution is positively skewed with a preponderance of lower values for $p < 0.3$. The histogram in Figure 2A has been fitted with a Γ density function

$$\Gamma(2,\lambda) = \frac{\lambda^2}{2} p e^{-\lambda p},$$

with $\lambda = 7.9$. For comparison, note that the distribution of release probabilities obtained by Allen and Stevens (1994) is well fitted by the same function with $\lambda = 7.2$.

In fact, we believe that we may have somewhat underestimated the number of synapses with very low probabilities for at least two reasons: (1) Low p synapses would be labeled weakly at best; weak staining is more difficult to detect. (2) Even if one or two vesicles were labeled and visualized, such weakly staining synapses were not included in the analysis unless the labeled vesicles were subsequently released during the destaining period; destaining might not occur effectively at low p synapses. We estimated the number of boutons with low release probability that were not detected with the usual 20–50 action potential loading as follows. In three experiments, after loading with 50 action potentials and obtaining the images of the labeled boutons, the boutons were further stained with FM1–43 using a stronger stimulus of 5 Hz for 30 s. This stimulation rate and duration was chosen to allow facilitation of low probability synapses without causing extensive depression of release from the higher probability synapses. After the more intense stimulation, the labeled terminals were visualized once more. On average, 18% more boutons were labeled after the strong stimulus than after the milder stimulus. The shape of the release probability distribution (after appropriately scaling the intensity axis) for the stronger stimulus did not, however, differ significantly from that obtained with milder stimulus ($p < 0.1$, Kolmogorov–Smirnov test). This observation indicates that the shape of the distribution that we obtained with the 50 action potential stimulus train was not significantly distorted by the inability to detect very low probability synapses, although we missed a fraction of the synapses present.

Distributions of release probabilities were obtained in 24 experiments with conventional and microdot cultures grown for 11–30 days; all distributions were similar to that illustrated in Figure 2A. Figure 2B shows the distribution of release probabilities estimated for 611 boutons from seven cells grown in conventional cultures for 11–15 days (these cells were selected for the similarity of recording conditions and number of days in vitro). The histogram has been fitted with a gamma density function $\Gamma(2, \lambda)$ with $\lambda = 11.1$.

Release Probability Distribution Obtained from FM1–43 Fluorescence Predicts MK–801 Blocking Curve

To compare our present technique with a previously used method for estimating the distribution of p, we studied the use-dependent block of NMDA responses by MK–801 (Hessler et al., 1993; Rosenmund et al., 1993) and determined the release probability distribution at

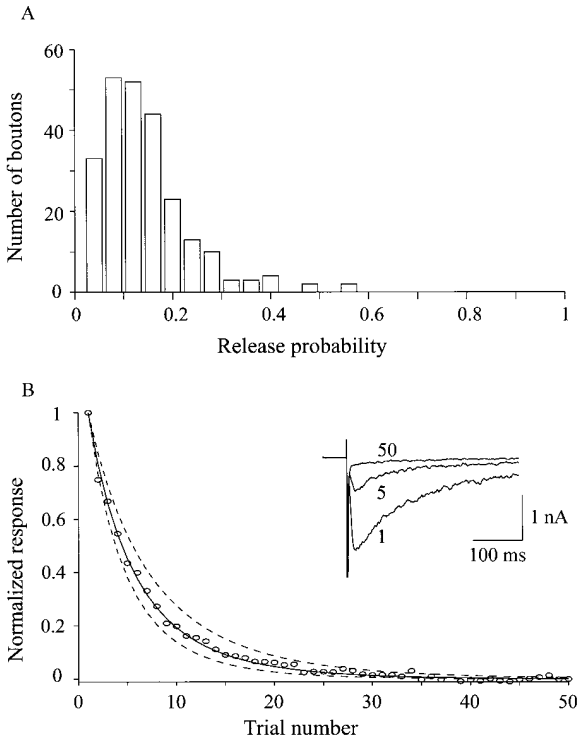

Figure 3. Release Probability Distribution Obtained from FM1–43 Loading Predicts MK–801 Blocking Curve

(A) The distribution of release probabilities obtained from 242 boutons in a single-neuron microisland. The boutons were labeled by stimulating the neuron at 0.5 Hz for 150 s (75 action potentials) in the presence of 10 μM FM1–43. During this stimulation, 10 μM MK–801 was also present, allowing the determination of rate of blocking of NMDA responses (see [B]). Subsequent to washing in dye-free medium for >5 min, the boutons were visualized. Action potentials were then evoked at 5 Hz for 3 min to completely destain the terminals. The total releasable fluorescence was measured for each bouton, and the distribution was scaled by the estimated single vesicle fluorescence intensity (87 intensity units for this experiment) to obtain the distribution of release probabilities.

(B) The rate of blocking of NMDA responses by MK–801. Autaptic NMDA currents were isolated by including 10 μM DNQX and 20 μM picrotoxin in the bathing medium and omitting Mg^{2+}. Autaptic currents were integrated and normalized to the first response (open circles). The response declined steadily and reached a small steady value. The final steady value, which could be due to unbinding of MK–801 from NMDA receptors, was subtracted from the response. Using the release probability distribution obtained from FM1–43, the MK–801 blocking curve could be predicted with $c = 87$ using equation (9) with no additional parameters (solid line). The dotted lines are predictions with $c = 65$, and $c = 109$.

the same set of synapses using FM–143 staining. These experiments were done with single neuron microislands, which allowed measurement of autaptic currents. The use of an isolated single neuron was essential so that we could be sure that the same population of synapses was studied electrophysiologically and with FM1–43.

NMDA receptor–mediated currents were isolated by blocking AMPA responses with 10 μM DNQX. Following a period of baseline measurement (10 trials), 75 action potentials were evoked at 0.5 Hz in the presence of 10 μM MK–801, which led to a progressive reduction in the NMDA response (Figure 3B, circles). During this period, 10 μM FM1–43 was present in the bathing medium. Subsequently, the neuron was washed with dye-free Ringer for >5 min and destained with action potentials evoked at 5 Hz. The distribution of fluorescence intensities of puncta was obtained as before. If the fluorescence intensities are scaled correctly to obtain the values of p (Figure 3A), then the distribution of p determined by FM1–43 loading should be sufficient to predict the MK–801 blocking curve completely, with no free parameters (Huang and Stevens, unpublished data; also see the Appendix). The scale factor used was $c = 87$ for this experiment. The MK–801 blocking curve predicted from the measured p distribution is shown as a solid line in Figure 3B and fits the actual data very well. Changing c by ±25% gives a clearly incorrect fit, and we should have detected an error in c of >∼10% (See Figure 3B). Similar results were obtained in three experiments in microislands. This concordance of results with two very different methods for estimating the p distributions provides strong support for our estimate of c (within ∼10%) and for the assumption (discussed later) that each release in the presence of FM1–43 is associated with adding a stained vesicle to the bouton's pool.

Paired-Pulse Modulation

To determine the extent and direction of changes in release probability that occur when a spike follows another within a short interval (Mallart and Martin, 1968), we compared the destaining kinetics at individual boutons for single and paired-pulse stimuli (50 ms interpulse interval). Previous studies have typically investigated paired-pulse modulation ("modulation" is used here to refer to either facilitation or depression) at populations of synapses, but such population studies cannot reveal any heterogeneity in synaptic responses to pulse pairs.

Figure 4A shows the changes in fluorescence intensity at two boutons during stimulation. The first four images were collected after FM1–43 staining of the terminals with 75 action potentials delivered at 0.5 Hz. These images were used to estimate the release probabilities as before (equation 1). Three more images were collected after delivering 25 single action potentials at 0.5 Hz. Then, 25 pairs of action potentials (50 ms interpulse intervals) were delivered at 0.5 Hz, and three more images were obtained. Finally, a long train of stimuli at 5 Hz was delivered to destain the terminals completely. Assuming that the release probability for the first action potential during paired stimulation is the same as that for the single action potential in the first period of stimulation, we can estimate p/N for the first and second action potentials using equation (2) to obtain

$$\frac{p_1}{N} = \frac{1}{k}\left(1 - \frac{\hat{F}_k}{\hat{F}_0}\right) \tag{4a}$$

$$\frac{p_2}{N} = \frac{1}{k}\left(1 - \frac{\hat{F}_{2k}}{\hat{F}_k}\right) - \frac{1}{k}\left(1 - \frac{\hat{F}_k}{\hat{F}_0}\right) \tag{4b}$$

Here, $\hat{F}_0$ is the initial fluorescence (a in Figure 4A); $\hat{F}_k$ is the fluorescence after k single action potentials (b in Figure 4A); and $\hat{F}_{2k}$ is the fluorescence after k single action potentials plus k paired action potentials (c in Figure 4A); p_1 is the release probability for the first pulse

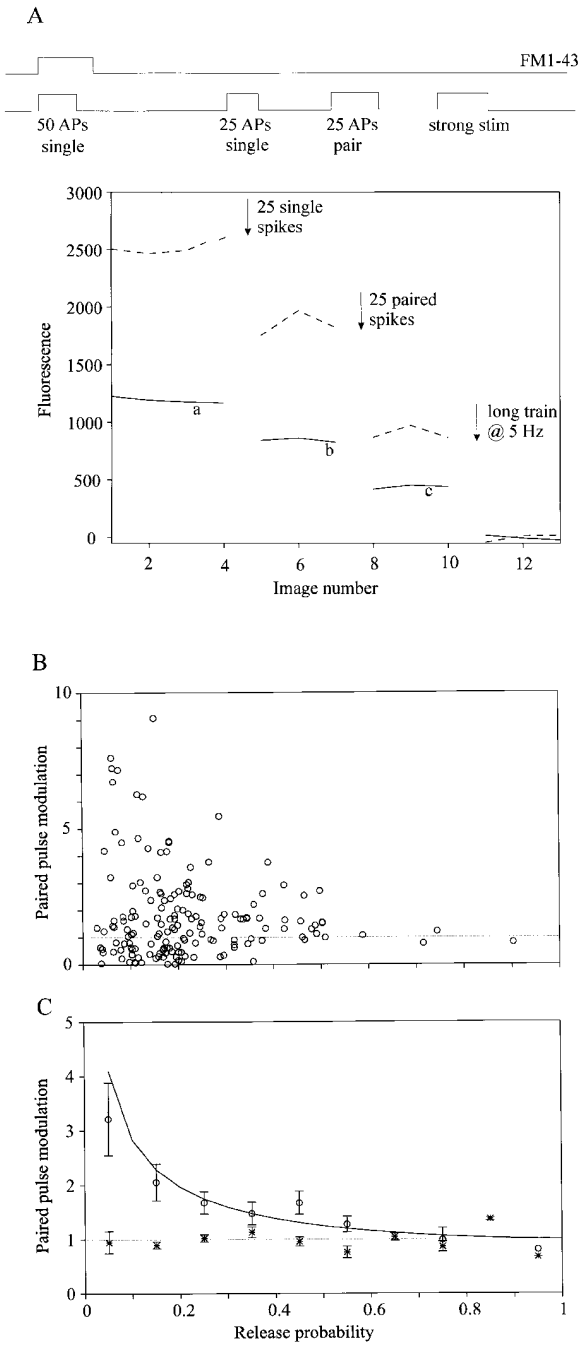

Figure 4. Paired-Pulse Modulation (PPM)

(A) Destaining curves for two typical boutons from a single cell. FM1–43 was loaded by stimulating the cell with 75 action potentials at 0.5 Hz. After four images were acquired, 25 single spikes were delivered at 0.5 Hz. After three more images were acquired, 25 spike pairs (50 ms separation between pairs) were delivered at 0.5 Hz. After three further images, a long train of 5 Hz stimulus was delivered to release all stained vesicles. The lines labeled a, b, and c represent the fluorescence intensities for a particular bouton. The ratios p_1/N and p_2/N were calculated as described in the text. The ratio of these two quantities gives the PPM. The release probability for each bouton was estimated from the initial fluorescence value.

(B) PPM values as a function of release probability for 166 boutons from three cells. The dotted line indicates the locus of PPM = 1.

(C) The PPM values were grouped in bins and averaged. The average and SEM are plotted at the midpoint of the corresponding bin (open circles). Note the difference in y-axis scale compared to (B). A general trend of decreasing PPM with increasing release probability can be seen (asterisks). In two other cells, destaining was done twice with single-pulse stimuli, and the ratios of the p/N for the two destaining runs were calculated as controls for the paired-pulse experiments. These values were binned and averaged as for the paired-pulse experiments (*). Note that these were uniformly scattered around 1 for all values of p. The solid line is given by

$$f(p) = \frac{1 - (1 - p)^{\frac{1}{\sqrt{p}}}}{p}.$$

of a pair, and p_2 is the release probability for the second pulse. Therefore, paired-pulse modulation can be obtained directly (without free constants) as the ratio of the right-hand side terms of the two equations above.

Paired-pulse modulation estimated this way varied widely across synapses (Figure 4B). To determine whether the magnitude of paired-pulse modulation was related to the initial release probability, we plotted the ratio of p_2/p_1 against the initial release probability that was estimated from distribution of initial fluorescence intensities as before. Although variability from synapse to synapse was considerable, on average, boutons with low initial probabilities were facilitated, and boutons with higher release probabilities were facilitated to a lesser extent and in some cases even depressed (Figure 4C). To determine the extent of variability caused by measurement error, in two experiments, we estimated p/N for each bouton from two successive destaining runs, each with identical stimulation protocol (50 single action potentials). The average ratio of the values of p/N calculated from the two destaining periods was plotted as a function of the release probability p (Figure 4C, control). This control ratio was close to 1 for all values of release probability, indicating that the trend seen for paired-pulse facilitation was not an artifact of the method used to estimate it.

The average facilitation across all boutons, irrespective of their initial p, was 2.07 $\pm$ 0.19 (SEM, N = 166). In earlier experiments in two cells, facilitation was measured for 72 boutons without an estimate for the initial release probability because the labeling with FM1–43 was done using a 5 Hz stimulus for 30 s. The average facilitation across the boutons was 2.18 $\pm$ 0.38, which is similar to that for data in Figure 4.

Dependence of Release Probability on External Calcium

Release probability is a function of the external calcium and is usually described by the Dodge–Rahamimoff power law (Dodge and Rahamimoff, 1967). While this dependence has previously been investigated for populations of synapses, with FM1–43 destaining, it becomes possible to investigate the relationship at individual boutons from a single neuron. One important issue that can be addressed is the following: How does the release probability at one calcium concentration depend on the release probability at another concentration? To investigate this question, we determined release probabilities at individual synaptic boutons in two external calcium concentrations.

As before, synapses were stained with FM1–43 with

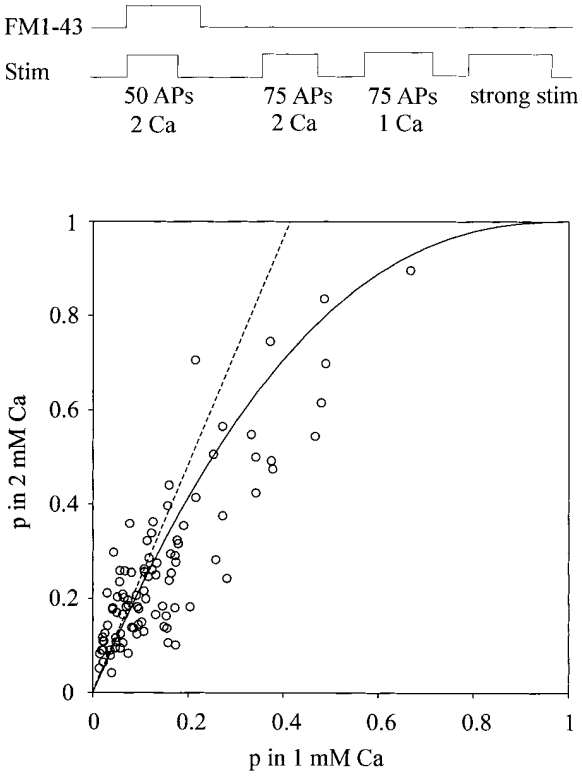

Figure 5. Dependence of Release Probability on External Calcium

A set of boutons were loaded with FM1–43 with 50 action potentials delivered at 0.5 Hz. Three images each were acquired before and after 50 action potentials evoked at 0.5 Hz with the external calcium concentration at 2 mM. The procedure was repeated for external calcium concentration of 1 mM (75 action potentials). Using equation (2), *p/N* was estimated for the two calcium concentrations. The value of *N* was estimated for each bouton from the value of *p/N* in 2 mM calcium, and *p* was estimated from loading. Therefore, the value of *p* in 1 mM Ca could also be estimated. The value of *p* in 2 mM is plotted against that for 1 mM Ca for 95 boutons from two cells. The solid line is given by the equation: $p(2) = 1 - (1-p[1])^{2.4}$. Note that the value of the release probability for the linear relation (dotted line) cannot exceed 1.

50 action potentials at 0.5 Hz in 2 mM calcium. With a protocol similar to that used to study paired-pulse facilitation, we estimated the relative release probabilities at different calcium concentrations (2 mM and 1 mM) by observing destaining at two calcium concentrations and using equation (2). Figure 5 shows release probabilities at the two calcium levels for 95 boutons from two cells.

According to the Dodge–Rahamimoff equation, the release probability *p(c)* at an extracellular calcium concentration *c* is related to the probability at concentration c_o by the ratio

$$\frac{p(c)}{p(c_0)} = \left(\frac{c\left(1 + \frac{c_0}{K_1} + \frac{1.3}{K_2}\right)}{c_0\left(1 + \frac{c}{K_1} + \frac{1.3}{K_2}\right)} \right)^4,$$

where K_1 and K_2 are constants and the extracellular concentration of magnesium is 1.3 mM, the value used in the experiments reported here. Typical values for the constants in this equation are $K_1 = .28$, and $K_2 = 1$ (with concentrations specified in mM; see Allen and Stevens, 1994); for our experiments, $c = 2$ mM, and $c_0 = 1$ mM. With these values, the ratio of probabilities should be $p(c)/p(c_0) = 2.4$. If all synapses were affected equally by the change in calcium concentration, independent of their release probability $p(c_o)$, then the straight line with a slope of 2.4 in Figure 5 would be predicted. Although this relation seems to hold for the values of $p(c_o)$ below $\sim$0.3, above that value, points tend to fall below the line predicted by the Dodge–Rahamimoff relation. Note that the Dodge–Rahamimoff equation cannot give release probabilities >1, but precisely how this restriction is implemented is not specified.

One explanation for the deviation from linearity is as follows. Schikorski and Stevens (unpublished data) have derived a relation between the release probability *p* and what they called the "exocytotic probability" *a*, the conditional probability that a vesicle will initiate exocytosis when a nerve impulse arrives, given that no other exocytotic event just occurred at that active zone:

$$p = 1 - e^{-an};$$

n is the number of vesicles in the readily releasable pool. This relation is derived from the assumption that, on the arrival of a presynaptic action potential, each of the *n* vesicles present has a probability *a* to initiate exocytosis, but as soon as the first exocytotic event starts, all other releases are forbidden; this is, according to their argument, why single active zones release at most one vesicle. Suppose that the exocytotic probability *a* follows the Dodge–Rahamimoff equation so that $a(2) = 2.4a(1)$, where the argument of *a* specifies the extracellular calcium concentration in mM. If the exocytotic probabilities followed this relationship, then the release probabilities would vary according to the equation

$$p(c) = 1 - (1 - p(c_0))^{2.4},$$

as can be seen after some simple algebraic manipulations. The curved relation on Figure 5 is a graph of this function. Thus, it appears that individual vesicles follow the Dodge–Rahamimoff equation, but synapses as a whole deviate from it at higher release probabilities.

Relation between Release Probability and the Recycling Pool of Vesicles

In experiments where loading and destaining were carried out under identical stimulation rates, an estimate for *N*, the size of the recycling pool of vesicles, could be obtained as the ratio of *p* and *p/N* from equation (3):

$$N = \frac{F_i k}{ci\left(1 - \frac{\hat{F}_k}{\hat{F}_0}\right)}.$$

All quantities on the right side of this equation are directly known from experiment except *c*, the fluorescence intensity per vesicle; selecting a value for *c* provides absolute estimates for *N*. Figure 6 shows the relation between *p* and *N* for 64 puncta from one cell: *N* and *p* are strongly correlated (correlation coefficient = 0.81; significance level <0.001). The axes in this figure

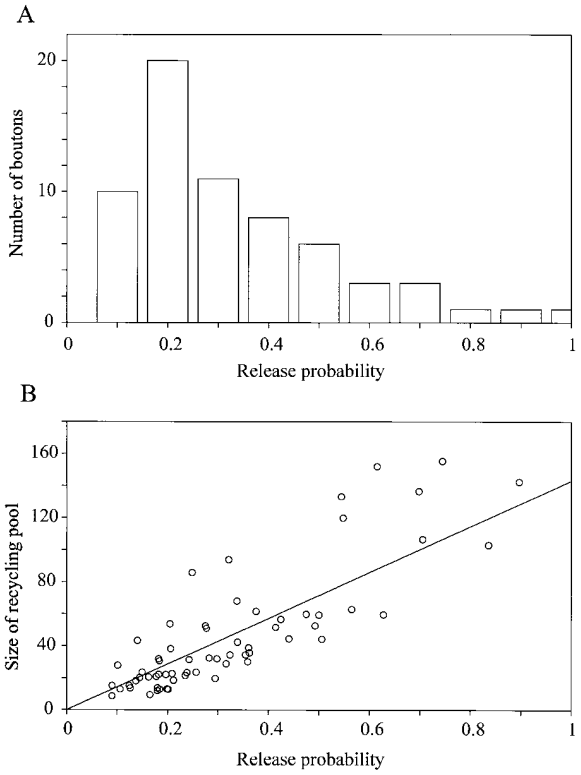

Figure 6. Relation between the Size of Recycling Pool and Release Probability

(A) Release probability distribution is shown for 64 boutons from one cell. Loading of FM1–43 was done with 50 action potentials evoked at 0.5 Hz. The distribution was scaled using a single vesicle fluorescence estimate of 102 units.

(B) The size of recycling pool *N* was determined as the ratio of *p* (estimated from initial fluorescence) and *p/N* determined from the destaining (equation 2). The resulting estimate was plotted against *p* for the 64 boutons (circles). The solid line is the best-fitting regression line passing through the origin. The correlation coefficient was 0.81 (significance level $<<$ 0.001).

were scaled using $c = 102$ intensity units as the estimate for the fluorescence of a single vesicle. Similar strong correlations ($R > 0.6$) were found in all 12 experiments in which loading and destaining were done at same rates of stimulation. The slope of the regression line corresponds to the recycling pool size for a synapse with $p = 1$ and was on average 115. Table 1 summarizes the data from these experiments.

Table 1. Correlation between Release Probability and Vesicle Pool Size

Cell Number	DIV*	Corr Coef	Maximum *N*
1	13	0.69	189
2	13	0.76	61
3	15	0.61	123
4	15	0.78	72
5	15	0.67	96
6	8	0.92	104
7	20	0.60	200
8	22	0.60	49
9	24	0.81	143
10	24	0.79	122
11	25	0.81	92
12	25	0.70	131
Mean		0.73 ± 0.10	115 ± 47

*Days in vitro

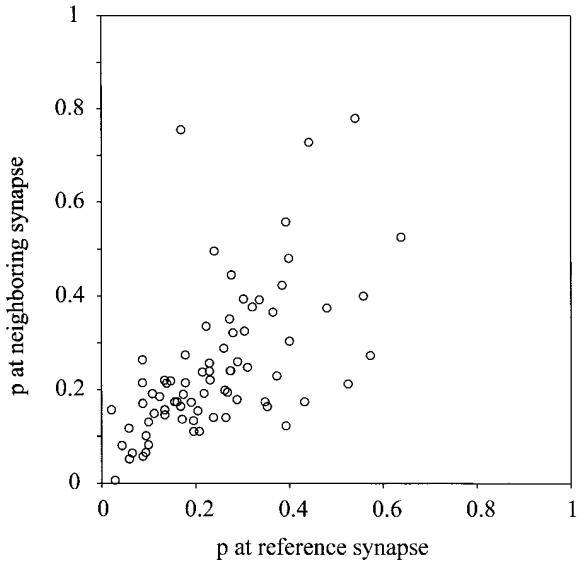

Figure 7. Release Probabilities at Neighboring Synapses Are Correlated

Strings of three or more puncta that were in a line were visually identified in five cells. The release probabilities for 76 pairs of adjacent puncta are shown. The correlation coefficient was 0.60 (significance level $<<$ 0.001). The correlation between randomly chosen pairs of synapses was 0.12 (significance level $>$ 0.2).

Release Probabilities at Neighboring Synapses Are Correlated

In some experiments, it was possible to discern strings of FM1–43 puncta that appeared to occur on the same dendrite. Since only the cell attached to the recording pipette was stimulated, all puncta also correspond to synapses formed by the same axon. The spacing between these puncta averaged ~3 μm, which is similar to that observed in immunostained preparations. We compared the release probabilities of immediately adjacent synapses from five cells (Figure 7). The correlation coefficient for this relation was 0.60, and the significance level was <0.001. This correlation diminished to 0.37 (significance level >0.1) when pairs separated by one intervening synapse were compared. The correlation coefficient for randomly chosen pairs of synapses was 0.12 (significance level >0.2).

Discussion

We have estimated the distribution of release probabilities for synapses made by a single cell and have found that several synaptic properties are quite variable from synapse to synapse but are highly correlated with release probability.

Character of the Release Probability Distribution

The experiments described here confirm previous suggestions that release probabilities fall on a continuous

rather than a bimodal distribution (Allen and Stevens, 1994; Huang and Stevens, unpublished data) and thus do not support the hypothesis that there are two distinct populations of synapses, one with low *p* and one with high *p* (Hessler et al., 1993; Rosenmund et al., 1993). Instead, we find that a wide range of values for *p* are represented even at synapses from the same axon, with a predominance of low *p*. In agreement with the observation first made by Rosenmund et al. (1993), we find heterogeneity in the release probabilities for synapses made by a single cell on a single target neuron.

Assumptions

One crucial assumption of the method used here is that for every vesicle released, a vesicle is endocytosed (and stained) over the period that dye is present. This supposition seems reasonable. Capacitance measurements at bipolar neuron synapses show a close match between exocytotic and endocytotic membrane areas. Von Gersdorff and Matthews (1994) and Smith and Betz (1996) found that the endocytotic internalization of FM1–43 stained membrane matches the quantity of exocytosis measured with the capacity measurement technique and with FM1–43 staining. The number of stained vesicles should therefore closely approximate the quantity of release. In our experiments, we used loading stimulus trains of 20–50 stimuli at a rate of 0.5 Hz. Thus, the characteristic time for endocytosis should fall between the 1–2 s time constant for single stimuli reported by Von Gersdorff and Matthews (1994) and the 30 s time constant found by (Ryan et al., 1996b), who used stimulus trains with higher rates than the ones used here. After the termination of stimulation, the FM1–43 was present in the solution for another 30 s, a sufficient time for the exocytosed vesicular membrane to be labeled and endocytosed (see Experimental Procedures). Unfortunately, no method is currently available for estimating the errors in the exocytosis–endocytosis match at single synapses, but the results of our MK–801 experiment place rather narrow limits on the errors in our estimates of release probability ($\pm$10%).

Another important assumption is that at most one vesicle is released per active zone for a single nerve impulse. This assumption is also likely to be valid because Stevens and Wang (1994, 1995) found single vesicle release per bouton with minimal stimulation in hippocampal slices, and Schikorski and Stevens (unpublished data) report that the majority of boutons have only one active zone. Nevertheless, the fraction of boutons that contain multiple active zones will be a source for some error. If multiple vesicles are released per impulse, we would overestimate the true *p*.

Analysis of Paired Modification

Short-term modification of *p* is thought to underlie certain forms of short-term synaptic plasticity (Magleby, 1987; Zucker, 1989; Stevens and Wang, 1995). Paired-pulse stimulation, a commonly used protocol for probing short-term synaptic plasticity, generally increased release probabilities for the second stimulus under conditions of our recordings. The amount of paired-pulse facilitation was high for synapses with low initial release probability and decreased with increasing *p*. This is partly expected from the simple observation that even if release probability for the second release = 1, paired-pulse facilitation would be $1/p$, which is a function that decreases with increasing *p*. In fact, a previous study using the minimal stimulation technique in slices found that for some synapses, the second release occurred reliably, independent of the value of *p* for the first pulse (Stevens and Wang, 1995). However, *p* estimated for the second pulse in our experiments did not approach 1 for most values, indicating that other factors need to be invoked to explain the dependence of paired-pulse facilitation on initial *p*. The response to paired-pulses is likely to be governed by a combination of several factors, including different forms of facilitation and depression (Magleby, 1987), and have been studied in hippocampal cultures electrophysiologically (Mennerick and Zorumski, 1995). Because these factors were not dissociated in our experiments, only a general conclusion can be reached. The consistency of our observations with electrophysiological studies of facilitation (Debanne et al., 1996), however, further strengthens the view that FM1–43 destaining in fact reflects the release probability.

For synapses with low *p*, considerable scatter was observed in the extent of paired-pulse modulation. Although part of this could reflect measurement error, it is likely that intrinsic biological variability at low *p* synapses contributed to the scatter (see also Ryan et al., 1996a). Synapses with low *p* are likely to be smaller. In fact, our experiments indicate a correlation between *p* and vesicle pool size (Figure 6B), which in turn is likely to be correlated with overall size of the synapse (Schikorski and Stevens, unpublished data). The small size of such synapses could lead to fluctuations in the entry of calcium following action potentials (Murthy et al., 1995, Soc. Neurosci. abstract; Frenguelli and Malinow, 1996; Mackenzie et al., 1996), which in turn could introduce variability in facilitation.

Spatial Correlations in Synapse Properties

Neighboring synapses tended to have similar release probabilities. If synaptic release probability is determined (at least in part) by patterns of activity in the pre- and postsynaptic elements, it is reasonable to suppose that synapses that are close to each other experience similar patterns. This similarity is likely to be strong for neighboring synapses formed by the same axon, on the same dendritic shaft. Although no correlation could be discerned for synapses (made by a single neuron) that were not immediate postsynaptic neighbors, further experiments are needed to determine the spatial extent over which release probabilities are correlated and to elucidate the mechanisms responsible.

Recycling Pool Size and Total Number of Vesicles per Bouton

We have shown that the size of the recycling pool *N* is proportional to the release probability; how is *N* related to the total number of vesicles per bouton? Schikorski and Stevens (unpublished data) report that the total number of vesicles per bouton averages 195 for boutons

in culture like the ones studied here. The average recycling pool for our experiments is 21 (average release probability = 0.18, and the proportionality constant between release probability and N is 115), so only ~10% of the total vesicles per bouton would participate in the recycling pool under the conditions of our experiments. This observation suggests that the reserve pool is not uniform but has multiple levels of accessibility. Clearly the factors that determine N and its relation to the total number of vesicles per bouton need to be elucidated.

In conclusion, we have estimated the distribution of release probabilities at synapses formed by a single presynaptic axon and find that it is continuous, broad, and skewed toward low probabilities. In addition, we present evidence for the possibility that release probability may be correlated with morphological features such as the pool size of synaptic vesicles and dendritic neighborhood. Our study can be extended to study the effect of a number of factors, including activity, on presynaptic function.

Experimental Procedures

Culture preparation: Hippocampal neurons were cultured using the methods described previously (Bekkers and Stevens, 1991). Cultures were allowed to mature for 10–25 days before recordings were made. For some experiments, microisland cultures were used (Bekkers and Stevens, 1991). For these, the substrate solution was sprayed on to coverslips using a glass microatomizer to form discrete spots. When neurons are grown on these coverslips, several of the microislands contained single neurons, which formed autapses and were then used for recording.

Electrophysiology: The whole-cell patch-clamp configuration was used to stimulate action potentials and to record autaptic currents. The patch pipette solution contained (in mM): 120 KGlu, 10 KCl, 5 Mg–ATP, 0.3 GTP, 10 HEPES, and 0.2 EGTA. Cells were perfused with extracellular medium containing (in mM): 136 NaCl, 2.5 KCl, 10 glucose, 10 HEPES, 2 $CaCl_2$ and 1.3 $MgCl_2$. In some experiments, the external Ca^{2+} concentration was varied, and these are indicated in the appropriate sections. For most recordings (except where mentioned), 10 μM DNQX and 50 μM D–APV (Research Biochemicals International) were included in the medium to prevent recurrent excitation and any potential activity-dependent changes in release probability. Action potentials were evoked by briefly stepping the voltage from −70 mV to +20 mV for 0.5 or 1 ms. Electrophysiological data were acquired with a Pentium 90 MHz computer (Dell) using National Instruments boards (AT-MIO-16 and AT-DIO-32) and software (Labview).

FM1–43 loading and destaining: Synaptic vesicles were loaded with the dye FM1–43 by bathing the cultures in medium containing 5–10 μM dye and eliciting 50 or 75 action potentials in the neurons at 0.5 Hz. We chose this stimulation rate, even though it is higher than those often used in electrophysiological studies, to avoid excessive background staining, which occurred due to longer exposure to dye, at rates slower than 0.5 Hz. Stimulation was then stopped, and the neurons were bathed in dye-containing medium for another 30 s to ensure maximal dye loading. The 30 s poststimulus loading time was chosen to be long enough to ensure that exocytosed vesicular membrane was retrieved but short enough to minimize background and nonspecific staining. In pilot experiments, we found that the number of stained vesicles was the same with a 30 s and a 2 min poststimulus loading time. We therefore standardized on the 30 s loading time to minimize artifactual staining. This was followed by at least 5 min of washing with dye-free medium. In some early experiments, loading of FM1–43 was achieved by stimulation at 5 Hz for 30 s.

Stimulating the neuron caused release of dye-containing vesicles, which was visualized as a loss of fluorescence. The total releasable fluorescence and the rate of loss of fluorescence were then used to estimate release probabilities and other related parameters (see Theory). Several protocols for destaining were used and are described in relevant sections.

MK–801 blocking experiments: In some experiments with neurons grown in microislands, NMDA receptor currents were isolated by leaving out D–APV and $MgCl_2$ in the bathing medium. AMPA and GABA currents were blocked with 10 μM DNQX and 20 μM picrotoxin, respectively. In these experiments, autaptic currents were monitored by whole-cell recordings (voltage clamp at −70 mV) and after obtaining a baseline synaptic response, 10 μM MK–801 was added to the perfusion medium. Successive stimulation caused blocking of the NMDA response. During this stimulation, which usually consisted of 50–75 action potentials at 0.5 Hz, 10 μM FM1–43 was present in the bathing medium to allow staining of the same synapses that were activated. The preparation was washed for >5 min in dye-free medium. After visualizing the stained boutons, they were destained using action potentials evoked at 5 Hz. Autaptic currents after each response were integrated to obtain total charge transferred to the soma. Charge contribution due to action currents was measured at the end of the experiment, after >600 action potentials were evoked in the continuous presence of MK–801. This charge was subtracted from all responses to isolate charge contributed by synaptic currents.

Imaging and analysis: Recordings were made on a Zeiss WL upright microscope with the recording chamber and electrode holders attached to a movable stage. Imaging was done using a BioRad MRC-600 confocal laser scanning microscope. The 488 nm line of the argon ion laser was used for excitation, and the emitted light was filtered through a 510 nm long-pass filter cube and detected by a photomultiplier. A second photomultiplier was used to detect the transmitted signal, which provided transmitted light images of the preparation. A 40×, 0.75 NA water-immersion objective (Zeiss) was used for imaging. Images were acquired by a PC using software provided by BioRad (SOM and MPL) at the rate of one frame (512 × 768 pixels or 256 × 256 pixels) every 15 s.

Images were analyzed using custom-written software in MATLAB. Regions of interest (ROI) around isolated bright spots were defined, and pixels within the ROI were integrated for each frame. Fluorescence is expressed in intensity units that correspond to fluorescence values integrated over all pixels within the ROI (fluorescence value for each pixel varied from 0–255). Since ROIs were defined by rectangles, they usually included a small background area. However, its contribution would be removed since in all experiments, the fluorescence value after complete destaining was subtracted from all frames. In a few experiments, slight shifts in successive images were sometimes observed. To account for these, the region of interest was shifted to be centered on the center of brightness of the fluorescent spot (Ryan and Smith, 1995). A few experiments, in which excessive shifts in images occurred presumably due to changes in focal distance, were discarded.

Appendix

A Simple Model for Labeling of Synaptic Vesicles with FM1–43

Loading Experiments

Let N be the average number of vesicles available for release at a given synapse. This includes the immediately releasable vesicles and the reserve pool. Let p be the probability of evoked vesicle release at that synapse; Stevens and Wang (1994, 1995) have shown that a single bouton can release at most one quantum of transmitter, so that the Katz (1969) N_s, the number of release sites per bouton, is 1. If labeling of vesicles is done using a low rate of stimulation (usually 0.5 Hz) with a 30 s poststimulus period with dye present, it is reasonable to assume that the number of endocytotic events is close to the number of vesicles released (Von Gersdorff and Matthews, 1994; Smith and Betz, 1996; Figure 2). A newly endocytosed vesicle will contain FM1–43 and is referred to as a stained vesicle. If each release is rapidly followed by an endocytotic event, the average number n of vesicles stained after the $(i+1)^{th}$ stimulus is related to the number stained after i^{th} stimulus by:

$$n_{i+1} = n_i + p\left(1 - \frac{n_i}{N}\right)$$

The factor $(1 - n_i/N)$ gives the conditional probability that an already stained vesicle will be released, given there is a release at all. Because endocytosis is not instantaneous (Ryan et al., 1996b), this equation provides an upper limit for the average number of stained vesicles. Since $n_0 = 0$ (no stained vesicles in the beginning), the difference equation

$$n_{i+1} = n_i\left(1 - \frac{p}{N}\right) + p$$

has the solution

$$n_i = N\left(1 - \left(1 - \frac{p}{N}\right)^i\right).$$

Expanding $(1-p/N)^i$ to first order for $p/N << 1$, we get

$$n_i = ip$$

(We return later to consider errors that result from our use of the $p/N << 1$ limit.) Therefore, after i action potentials, the number of labeled vesicles is proportional to the probability of release. If we assume that different labeled vesicles contain similar amounts of dye, then the fluorescence intensity will be proportional to release probability, and we have

$$F_i = cip$$

or

$$p = \frac{F_i}{ci}, \tag{1}$$

where c is a factor corresponds to the fluorescence intensity of a single vesicle. Therefore, the distribution of fluorescence intensity of boutons following a staining protocol is identical to the distribution of release probabilities up to a scale factor. Estimates of and accuracy limits for the scale factor c were obtained as described in the Results section.

Destaining Experiments

After loading with FM1–43, let the number of dye-filled vesicles be n_0. During destaining of the terminals, the number of stained vesicles after the $(k+1)^{th}$ stimulus is

$$n_{k+1} = n_k - p\frac{n_k}{N - u_k},$$

where u_k is the number of vesicles released on the first k stimuli that have not been returned to the available pool whose size is N; we assume that once a vesicle is returned to the pool, it is well mixed in the sense of Ryan and Smith (1995). Following the $(k+1)^{th}$ stimulus, then, an average of $pn_k/(N-u_k)$ stained vesicles will be released per bouton (that is, one stained vesicle will be released per bouton with probability $pn_k/[N-u_k]$). The problem is that the number of vesicles that have been released and not returned to the pool drawn upon for release (the quantity u_k) is unknown and cannot be measured with our experimental protocol. It turns out, however, that u_k can, to an excellent approximation, be neglected for our experiments. We now turn to a derivation of the approximate relationship needed for the interpretation of our destaining experiments.

Divide the difference equation above by the initial number of stained vesicles (after loading), n_0, to give

$$\frac{n_{k+1}}{n_0} = \frac{n_k}{n_0}\left(1 - \frac{p}{N - u_k}\right).$$

Now call f_k the estimate of n_k/n_0 obtained when u_k is assumed to be zero, and φ_k is the estimate when $u_k = kp$, its maximum possible value (neglecting spontaneous release at the synapse). Thus, we can place the bounds on n_k/n_0

$$f_k \geq \frac{n_k}{n_0} \geq \varphi_k;$$

our strategy is to show that, for the conditions of our experiments, the equality holds in the preceding equation so that

$$f_k \approx \varphi_k \approx \frac{n_k}{n_0}.$$

The difference equations that describe these two bounding cases are

$$f_{k+1} = f_k\left(1 - \frac{p}{N}\right)$$

and

$$\varphi_{k+1} = \varphi_k\left(1 - \frac{p}{N - kp}\right) = \varphi_k\left(1 - \frac{\frac{p}{N}}{1 - k\frac{p}{N}}\right).$$

Note that the two limiting cases correspond to the limits of very rapid and very slow recyling of vesicles: the equation for f_k describes the case of very rapid (instantaneous on a 2 s timescale) endocytosis, and the equation for φ_k holds exactly for very slow (zero rate on a 2 min timescale) endocytosis.

The solutions to these equations (with the initial value 1) are

$$f_k = \left(1 - \frac{p}{N}\right)^k$$

and

$$\varphi_k = \left(1 - \frac{p}{N}k\right)$$

The bounds on n_k/n_0 are then

$$f_k = \left(1 - \frac{p}{N}\right)^k \geq \frac{n_k}{n_0} \geq \left(1 - \frac{p}{N}k\right) = \varphi_k.$$

When this inequality is solved for p/N, we obtain

$$1 - \left(\frac{n_k}{n_0}\right)^{\frac{1}{k}} \geq \frac{p}{N} \geq \frac{1}{k}\left(1 - \frac{n_k}{n_0}\right).$$

The ratio n_k/n_0 also equals the ratio $\hat{F}_k/\hat{F}_0$ of the fluorescence $\hat{F}_k$ after k stimuli to the initial fluorescence $\hat{F}_0$. Therefore, the term p/N is bounded by two measurable quantities:

$$1 - \left(\frac{\hat{F}_k}{\hat{F}_0}\right)^{\frac{1}{k}} \geq \frac{p}{N} \geq \frac{1}{k}\left(1 - \frac{\hat{F}_k}{\hat{F}_0}\right).$$

For our experiments, the ratio $\hat{F}_k/\hat{F}_0$ is always close to 1, so that the upper bound in the inequality can be approximated as the first term in the expansion

$$1 - \left(\frac{\hat{F}_k}{\hat{F}_0}\right)^{\frac{1}{k}} = 1 - \left(1 - 1 + \frac{\hat{F}_k}{\hat{F}_0}\right)^{\frac{1}{k}} \approx \frac{1}{k}\left(1 - \frac{\hat{F}_k}{\hat{F}_0}\right)$$

because $1 - \frac{\hat{F}_k}{\hat{F}_0}$ is small. Since the upper and lower bounds of p/N are the same to first order in a small parameter $(1 - \hat{F}_k/\hat{F}_0$, we have the approximate expression

$$\frac{p}{N} = \frac{1}{k}\left(1 - \frac{\hat{F}_k}{\hat{F}_0}\right). \tag{2}$$

If staining and destaining are carried out at the same stimulus frequencies, p is the same under the two conditions for any given bouton. Therefore, the value of N for each bouton can be estimated as the ratio of p and p/N.

Magnitude of Errors Arising from the Approximations

Equations (1) and (2) for interpreting the loading and destaining experiments are approximations obtained by taking the first order term of an expansion around a small parameter. The exact equation that led to the approximate equation (1) is

$$n_i = N\left(1 - \left(1 - \frac{p}{N}\right)^i\right) = N\left(i\frac{p}{N} + \frac{i(i-1)}{2}\frac{p^2}{N^2} + \ldots\right)$$

$$\approx ip + \frac{(ip)^2}{2N}$$

For the experiments described, the relative error in our estimate of

p from equation (1) is ~5%. Experiments that use the procedure load/measure/load/measure reveal that intensity is in fact proportional to number of stimuli for twice the number of stimuli that we used in the loading experiments. Such experiments confirm that our error estimates are accurate, since an appreciable correction term would cause departures from linearity.

A similar analysis yields an error estimate for equation (2), and we find that the error in p/N is <10%.

The Distribution of Fluorescence Intensities for a Population of Boutons

The goal of this section is to calculate the distribution of intensities around the mean for a population of boutons, each of which contains n stained vesicles. The average intensity of a single stained vesicle is defined to be c intensity units, so the mean bouton fluorescence intensity F for the population is

$$F = cn.$$

Because of the source of variance evaluated below, individual boutons will have an intensity f that departs from the mean F; we calculate the distribution of f here.

Measurement error is the dominant source of variance in estimating intensity of bouton staining. We find that if the intensity of the same puncta is measured repeatedly, the intensity values fluctuate from measurement to measurement. The sources of this variability include photon counting noise, digitization errors, and fluctuations in the power output of the exciting laser. Experimentally, the SD of these measurements is linearly related to the mean—this is what would be expected if fluctuations in the laser power were the dominant noise source—with a coefficient of variation of 0.17; we denote the coefficient of variation in the measurement errors by v in the following.

The distribution of intensities for a population of boutons, each with n stained vesicles, is thus approximately normally distributed with a variance σ^2 determined by the measurement error:

$$\sigma^2 = \frac{(vnc)^2}{s},$$

where s is the number of samples (frames) averaged to estimate the intensity of each bouton. The SD of the intensity distribution for the population is thus

$$\begin{aligned}\sigma &= \sqrt{\frac{(vnc)^2}{s}} \\ &= \sqrt{\frac{v^2}{s}}\, nc \\ &= \sqrt{\frac{v^2}{s}}\, F,\end{aligned}$$

where F is the average intensity for the population. The coefficient of variation θ for the distribution of intensities f is therefore

$$\theta = \sqrt{\frac{v^2}{s}}.$$

For our experiments, $s = 4$, and $v = 0.17$. Therefore, the coefficient of variation θ is given, for a population of boutons, each with n stained vesicles, by

$$\theta = .085.$$

The probability $p_n(f)$, then, of finding fluorescence intensity f for a bouton containing n vesicles is

$$p_n(f) = \frac{1}{\sqrt{2\pi}cn\theta}\, e^{-\frac{(f-nc)2}{2c2n2\theta2}}$$

where c is the mean fluorescence of a single vesicle. For the i^{th} bouton, the probability $p(f_i)$ of finding an intensity f_i therefore is

$$p(f_i) = \sum_{n=1}^{N_v} w_n p_n(f_i)$$

where w_n is the probability that a bouton will contain n stained vesicles, and N_v is the maximum possible number of stained vesicles for a bouton.

Relating the MK–801 Blocking Equation with FM1–43 Distribution

Huang and Stevens (unpublished data) have derived an equation describing the successive NMDA responses of synapses in the presence of MK–801. If S_i is the NMDA response for stimulus i, then

$$S_i = \int_0^\infty pw(p)e^{-ip}\, .dp$$

where i denotes the stimulus number, and $w(p)$ is the release probability density function. We can approximate $w(p)$ with the experimentally determined histogram of release probabilities, $h(j\Delta x)$, where j is the bin number ranging from 1 to M, and x is the bin width. Therefore,

$$S_i \propto \sum_{j=1}^{M} j\Delta x h(j\Delta x)e^{-ij\Delta x}\Delta x \qquad (9)$$

This proportionality will become an equation when normalized by the value of S_1.

Acknowledgments

We thank Christopher Boyer for preparation of cell cultures. This work was supported by Howard Hughes Medical Institute (C. F. S. and T. J. S.), National Institutes of Health grants NS 12961 (C. F. S.) and R1MH46482A (T. J. S), and by a Helen Hay Whitney Foundation fellowship (V. N. M.).

Received September 23, 1996; revised March 3, 1997.

References

Allen, C., and Stevens, C.F. (1994). An evaluation of causes for unreliability of synaptic transmission. Proc. Natl. Acad. Sci. USA *91*, 10380–10383.

Bekkers, J.M., and Stevens, C.F. (1991). Excitatory and inhibitory autaptic currents in isolated hippocampal neurons maintained in cell culture. Proc. Natl. Acad. Sci. USA *88*, 7834–7838.

Betz, W.J., and Bewick, G.S. (1992). Optical analysis of synaptic vesicle recycling at the frog neuromuscular junction. Science *255*, 200–203.

Betz, W.J., Mao, F., and Bewick, G.S. (1992). Activity-dependent fluorescent staining and destaining of living vertebrate motor nerve terminals. J. Neurosci. *12*, 363–375.

Bolshakov, V.Y., and Siegelbaum, S.A. (1995). Regulation of hippocampal transmitter release during development and long-term potentiation. Science *269*, 1730–1734.

Debanne, D., Guerineau, N.C., Gahwiler, B.H., and Thompson, S.M. (1996). Paired-pulse facilitation and depression at unitary synapses in rat hippocampus: quantal fluctuation affects subsequent release. J. Physiol. (Lond.) *491*, 163–176.

Dodge, F.A., and Rahamimoff, R. (1967). Co-operative action of calcium ions in transmitter release at neuromuscular junction. J. Physiol. *193*, 419–432.

Frenguelli, B.G., and Malinow, R. (1996). Fluctuations in intracellular calcium responses to action potentials in single en passage presynaptic boutons of layer V neurons in neocortical slices. Learning Mem. *3*, 150–159.

Henkel, A.W., Lubke, J., and Betz, W.J. (1996). FM1–43 dye ultrastructural localization in and release from frog motor nerve terminals. Proc. Natl. Acad. Sci. USA *93*, 1918–1923.

Hessler, N.A., Shirke, A.M., and Malinow, R. (1993). The probability of transmitter release at a mammalian central synapse. Nature *366*, 569–572.

Heuser, J.E., Reese, T.S. (1973). Evidence for recycling of synaptic vesicle membrane during transmitter release at the frog neuromuscular junction. J. Cell Biol. *57*, 315-344.

Katz, B. (1969). The release of neurotransmitter substance. (Liverpool, United Kingdom: Liverpool University Press).

Mackenzie, P.J., Umemiya, M., and Murphy, T.H. (1996). Ca2+ imaging of CNS axons in culture indicates reliable coupling between

single action potentials and distal functional release sites. Neuron *16*, 783–795.

Magleby, K.L. (1987). Short-term changes in synaptic efficacy. In Synaptic Function, G.M. Edelman, W.E. Gall, and W.M. Cowan, eds. (New York: John Wiley and Sons), pp. 21–56.

Mallart, A., and Martin, A.R. (1968). The relation between quantum content and facilitation at the neuromuscular junction of the frog. J. Physiol. (Lond.) *196*, 593–604.

Mennerick, S., and Zorumski, C.F. (1995). Paired-pulse modulation of fast excitatory synaptic currents in microcultures of rat hippocampal neurons. J. Physiol. (Lond.) *488*, 85–101.

Raastad, M., Storm, J.F., and Andersen, P. (1992). Putative single quantum and single fibre excitatory postsynaptic currents show similar amplitude range and variability in rat hippocampal area CA1. Eur. J. Neurosci. *4*, 113–117.

Rosenmund, C., and Stevens, C.F. (1996). Definition of the readily releasable pool of vesicles at hippocampal synapses. Neuron *16*, 1197–1207.

Rosenmund, C., Clements, J.D., and Westbrook, G.L. (1993). Nonuniform probability of glutamate release at a hippocampal synapse. Science *262*, 754–757.

Ryan, T.A., and Smith, S.J. (1995). Vesicle pool mobilization during action potential firing at hippocampal synapses. Neuron *14*, 983–989.

Ryan, T.A., Reuter, H., Wendland, B., Schweizer, F.E., Tsien, R.W., and Smith, S.J. (1993). The kinetics of synaptic vesicle recycling measured at single presynaptic boutons. Neuron *11*, 713–724.

Ryan, T.A., Ziv, N.E., and Smith, S.J. (1996a). Potentiation of evoked vesicle turnover at individually resolved synaptic boutons. Neuron *17*, 125–134.

Ryan, T.A., Smith, S.J., and Reuter, H. (1996b). The timing of synaptic vesicle endocytosis. Proc. Natl. Acad. Sci. USA *93*, 5567–5571.

Smith, C.B., and Betz, W.J. (1996). Simultaneous independent measurement of endocytosis and exocytosis. Nature *380*, 531–534.

Stevens, C.F., and Wang, Y. (1994). Changes in reliability of synaptic function as a mechanism for plasticity. Nature *371*, 704–707.

Stevens, C.F., and Wang, Y. (1995). Facilitation and depression at single central synapses. Neuron *14*, 795–802.

Thomson, A.M., Deuchars, J., and West, D.C. (1993). Large, deep layer pyramid–pyramid single axon EPSPs in slices of rat motor cortex display paired pulse and frequency-dependent depression, mediated presynaptically and self-facilitation, mediated postsynaptically. J. Neurophysiol. *70*, 2354–2369.

Von Gersdorff, H., and Matthews, G. (1994). Dynamics of synaptic vesicle fusion and membrane retrieval in synaptic terminals. Nature *367*, 735–739.

Zucker, R.S. (1989). Short-term synaptic plasticity. Annu. Rev. Neurosci. *12*, 13–31.